APOE-ε4 risk variant for Alzheimer's disease modifies the association between cognitive performance and cerebral morphology in healthy middle-aged individuals

Raffaele Cacciaglia[a], José Luis Molinuevo[a,b,c,*], Carles Falcón[a,d], Gonzalo Sánchez-Benavides[a], Nina Gramunt[a,c], Anna Brugulat-Serrat[a], Manel Esteller[e,f,g], Sebastián Morán[e], Karine Fauria[a], Juan Domingo Gispert[a,d,h,*], for the ALFA study

[a] Barcelonaβeta Brain Research Center, Pasqual Maragall Foundation, Barcelona, Spain
[b] Institut d'Investigacions Biomèdiques August Pi i Sunyer (IDIBAPS), Barcelona, Spain
[c] CIBER Fragilidad y Envejecimiento Saludable (CIBERFES), Madrid, Spain
[d] Centro de Investigación Biomédica en Red de Bioingeniería, Biomateriales y Nanomedicina (CIBER-BBN), Madrid, Spain
[e] Cancer Epigenetics and Biology Program (PEBC), Bellvitge Biomedical Research Institute (IDIBELL), L'Hospitalet, Barcelona, Spain
[f] Physiological Sciences Department, School of Medicine and Health Sciences, University of Barcelona (UB), L'Hospitalet, 08908 Barcelona, Spain
[g] Institució Catalana de Recerca i Estudis Avançats (ICREA), Barcelona, Spain
[h] Universitat Pompeu Fabra, Barcelona, Spain

ARTICLE INFO

ABSTRACT

The APOE-ε4 genotype is the highest genetic risk factor for Alzheimer's disease (AD). In cognitively unimpaired individuals, it has been related to altered brain morphology, function and earlier amyloid beta accumulation. However, its impact on cognitive performance is less evident. Here, we examine the impact of APOE-ε4 allele load in modulating the association between cognitive functioning and brain morphology in middle-aged healthy individuals. A high-resolution structural MRI scan was acquired and episodic memory (EM) as well as executive functions (EFs) were assessed in a sample of 527 middle-aged unimpaired individuals hosting a substantial representation of ε4-homozygous (N = 64). We adopted a voxel-wise unbiased method to assess whether the number of APOE-ε4 alleles significantly modified the associations between gray matter volumes (GMv) and performance in both cognitive domains.

Even though the APOE-ε4 allele load did not exert a direct impact on any cognitive measures, it reversed the relationships between GMv and cognitive performance in a highly symmetrical topological pattern. For EM, interactions mapped onto the inferior temporal gyrus and the dorsal anterior cingulate cortex. Regarding EFs, significant interactions were observed for processing speed, working memory, and visuospatial attention in distinct brain regions. These results suggest that APOE-ε4 carriers display a structure-function association corresponding to an older age than their chronological one. Our findings additionally indicate that APOE-ε4 carriers may rely on the integrity of multiple compensatory brain systems in order to preserve their cognitive abilities, possibly due to an incipient neurodegeneration. Overall this study provides novel insights on the mechanisms through which APOE-ε4 posits an increased AD risk.

1. Introduction

Alzheimer's disease (AD) is a severe neurodegenerative disorder characterized by diffuse brain atrophy along with progressive decline in multiple cognitive domains. In recent years, the pathophysiological model of AD has been redefined along a disease continuum where the neuropathological changes, such as cerebral amyloid beta (Aβ) deposition, have been shown to precede any detectable cognitive manifestation by two or three decades (Sperling et al., 2014). Therefore, tremendous effort has been made in order to elucidate the link between the pathological cascade of AD and the emergence of cognitive symptoms (Jack Jr. et al., 2018).The APOE-ε4 allele represents the major genetic risk factor for sporadic AD by lowering the age of onset in a gene dose-dependent manner (Liu et al., 2013). APOE-ε4 codes the

apolipoprotein-ε4 (apoE4), which compared to other isoforms, is less effective in maintaining cerebral lipid homeostasis and in breaking down amyloid beta (Aβ) peptide, thus facilitating the formation of extracellular insoluble oligomers (Zhao et al., 2017). Cognitively intact *APOE*-ε4 carriers show higher cerebral Aβ deposition (Jansen et al., 2015; Reiman et al., 2009) as well as lower cerebral metabolism (Reiman et al., 2005), with these effects being proportional to the number of ε4 alleles. Previous studies have also reported an impact of the risk variant on cerebral morphology in healthy individuals (Alexander et al., 2012; Honea et al., 2009; Ten Kate et al., 2016) although this has not always been confirmed (Protas et al., 2013; Mondadori et al., 2007; Gonneaud et al., 2016; see Fouquet et al., 2014 for a review). Recently, using a spatially unbiased voxel-wise approach in a sample harboring a high number of healthy *APOE*-ε4 homozygous, we have reported dose–dependent effects of the risk allele on the volume of several AD-sensitive areas (Cacciaglia et al., 2018a). Yet, the underlying mechanisms through which *APOE*-ε4 posits increased risk for AD are not fully understood, and its impact on cognitive performance in unaffected individuals remains unclear. Previous seminal works reported a gene dose-dependent lifetime decline in episodic memory (EM) (Caselli et al., 2009) but not in executive functions (EFs) (Caselli et al., 2011) in cognitively unimpaired *APOE*-ε4 carriers compared to non-carriers, even though other studies could not confirm such a longitudinal association (Bunce et al., 2014). Similarly, cross-sectional studies reported either worse (Nao et al., 2017; Honea et al., 2009), better (Mondadori et al., 2007), or equivalent (Matura et al., 2016; Reiman et al., 2004) cognitive functioning in healthy carriers of the risk allele compared to non-carriers. Divergence among studies may depend on the age of the participants (Jochemsen et al., 2012) as well as the amyloid status, since the detrimental impact of *APOE*-ε4 in healthy individuals has been shown to occur in Aβ-positive individuals only (Lim et al., 2018).

Besides genetic liability, the greatest unmodifiable AD risk factor is represented by advanced age. Recently we have reported that, irrespective of the *APOE* status, aging modulates the relationship between cognitive performance (*i.e.*, both EM and EFs) and regional brain volumes in healthy participants, with older individuals displaying reversed associations compared to younger ones in medial temporal and prefrontal areas (Cacciaglia et al., 2018b). Since *APOE*-ε4 has been proposed to confer an accelerated aging process (Cacciaglia et al., 2018a; Evans et al., 2014; Filippini et al., 2011), one possibility is that, although not significantly affecting cognitive performance in the healthy population, the ε4 allele would modify the association between cognitive performance and the underlying brain morphology in a similar way as exerted by aging. This assumption is also supported by earlier functional neuroimaging studies which showed that *APOE*-ε4 modulates the relationship between cognitive performance and patterns of brain activity (Matura et al., 2016; Evans et al., 2014; Filippini et al., 2011; Bondi et al., 2005; Bookheimer et al., 2000) as well as cerebral Aβ deposition in healthy individuals (Kantarci et al., 2012).

In the present study we sought to determine whether this modulatory role is extendable to the brain structural level. We predicted that *APOE*-ε4 would shift the associations between regional GMv and cognitive performance in both EM and EFs. We tested our hypotheses on a sample of middle-aged cognitively healthy individuals which was enriched for the genetic risk for AD, hosting a significantly higher number of *APOE*-ε4 homozygous than previously reported in single-site neuroimaging studies of healthy subjects (*N* = 64). This sample characteristic allowed us testing separate genotypic models which may capture distinct biological pathways for the risk allele to confer AD liability, as previously suggested in structural neuroimaging studies of AD patients (Filippini et al., 2009) and healthy controls (Cacciaglia et al., 2018a).

2. Methods

2.1. Study participants

All subjects were enrolled in the ALFA (ALzheimer and FAmilies) study (Clinicaltrials.gov Identifier: NCT01835717), a large cohort program pointing to the identification of pathophysiological alterations in preclinical AD comprising 2743 study participants (Molinuevo et al., 2016). Participants were cognitively unimpaired with a Clinical Dementia Rate score of 0. Subjects with disorders which could interfere with cognition or with a psychiatric diagnosis were excluded from the study. Additional exclusion criteria have been described in detail previously (Molinuevo et al., 2016). After *APOE* genotyping, all participants homozygous for the ε4 allele as well as carriers of the ε2 allele were invited to undergo magnetic resonance imaging (MRI) scanning along with ε4-heterozygous and non-carriers matched for age and sex. This recruitment strategy resulted in 576 study participants, out of which 43 had to be discarded due to MRI incidental findings or poor image quality. From the remaining 533 individuals, 6 subjects were discarded due to missing cognitive data, yielding to a final sample of 527 subjects. For the statistical analyses participants were pooled according to the cumulative presence of the ε4 allele, that is in non-carriers (NC), ε4-heterozygous (HE) and ε4-homozygous (HO). The study was approved by the local ethics committee, and all participants gave written informed consent to participate in the study.

2.2. APOE genotyping

Total DNA was obtained from blood cellular fraction by proteinase K digestion followed by alcohol precipitation. Samples were genotyped for two single nucleotide polymorphisms (SNPs), rs429358 and rs7412, determining the possible APOE isoforms: ε1, rs429358 (C) + rs7412 (T); ε2, rs429358 (T) + rs7412 (T); ε3, rs429358 (T) + rs7412 (C); and ε4, rs429358 (C) + rs7412 (C). Of the 527 participants, 162 were ε3/ε4 carriers, 149 were homozygous for the ε3 allele, 104 were ε2/ε3 carriers, 64 were homozygous for the ε4 allele, 42 were ε2/ε4, and 6 were ε2/ε2 carriers. The allele frequencies did not significantly deviate from Hardy-Weinberg equilibrium ($\chi^2 = 5.99$, $p = .20$).

2.3. Image data acquisition and preprocessing

Magnetic resonance imaging (MRI) was conducted with a 3 T General Electric scanner (GE Discovery MR750 W). Structural 3D high-resolution T$_1$-weighted images were collected using a fast spoiled gradient-echo (FSPGR) sequence implementing the following parameters: voxel size = 1 mm³ isotropic, Repetition Time (TR) = 6.16 ms, Echo Time (TE) = 2.33 ms, inversion time (TI) = 450 ms, matrix size = 256 × 256 × 174, flip angle = 12°. Gray matter (GM) was segmented from images using the new segment function implemented in Statistical Parametrical Mapping software (SPM 12, Wellcome Department of Imaging Neuroscience, London, UK), and located into a common space for subsequent normalization using a 12-affine parameter transformation. Segmented GM images were used to generate a reference template of the sample, which was warped into a standard Montreal Neurological Institute (MNI) space using the high dimensional DARTEL toolbox (Ashburner, 2007). The generated flow fields and normalization parameters were then implemented to normalize the native GM images to the MNI space. In order to preserve the native local amount of GM volume, we applied a modulation step, where each voxel signal's intensity was multiplied by the Jacobian determinants derived from the normalization procedure (Good et al., 2001). Quality control of normalization was assured by checking the sample homogeneity with the computational anatomy toolbox (CAT12) (http://dbm.neuro.uni-jena.de/cat/) using non-smoothed data, which did not return errors in the registration procedure in any subject. Finally, images were spatially smoothed with a 6 mm full-width at half maximum (FWHM) Gaussian

kernel. Total intracranial volume (TIV) was computed by summing the segmented GM, white matter (WM) and cerebrospinal fluid (CSF) volumes for each individual.

2.4. Neuropsychological evaluation

The neuropsychological assessment took place on average 10.6 months (SD = 5.81) before the MRI session. EM was assessed using the Spanish adapted version of the Memory Binding Test (MBT) (Gramunt et al., 2016), an instrument that was developed for detecting subtle memory impairment in the cognitively intact population (Buschke, 2014). Previous studies have demonstrated the ability of the MBT (formerly referred as Memory Capacity Test [MCT]) to discriminate subjects with cerebral Aβ deposition (Papp et al., 2015), and to successfully predict the incidence of MCI longitudinally (Mowrey et al., 2016). During administration, subjects sequentially learn two lists of 16 words written in cards, where each card contains four words. The lists share semantic categories, which are used both to control the encoding of the words in learning and as cues during cued recall trials. After the presentation of each list, immediate cued recall (CR) of the presented items is tested, to provide a measure of successful encoding. Four main outcomes are produced: Total Paired Recall (TPR), which is the recall of both lists after semantic cueing; Total Free Recall (TFR), for the free recall of both lists; Total Delayed Paired Recall (TDPR), for the delayed (30 min after initial recall) after semantic cueing; and Total Delayed Free Recall (TDFR), for the delayed counterpart of the free recall. As a measure of cued memory retention, we computed the percentage of loss of learnt words over to two different time-laps. This was achieved by dividing TPR and TDPR scores by scores for immediate cued recall (CR), respectively. This procedure generated two different retention index scores: short-delay retention (SDR) and long-delay retention (LDR). The former (SDR) covered a time-lap of approximately 5 min (*i.e.*, the time between the end of CR and the last recalled word in TPR), while the latter (LDR) covered a lap of approximately 30 min (*i.e.*, the time between the end of CR and the last recalled word in TDPR).

EFs were assessed using the Wechsler Adult Intelligence Scale-Fourth Edition (WAIS-IV, Wechsler, 2012). We administered five subtests: Coding (cognitive processing speed), Digit Span (working memory), Matrix Reasoning (non-verbal problems solving), Visual Puzzles (visuospatial processing), and Similarities (verbal reasoning and abstract thinking). Digit Span subtests were studied separately as previously recommended (Colom et al., 2007) (Digit-span forward, Digit-span backward, Digit-span sequencing).

2.5. Statistical analysis

Group differences in demographic variables were assessed with a one-way analysis of variance or a chi-squared test for continuous or categorical variables, respectively.

To assess group differences in cognitive performance we conducted an analysis of covariance (ANCOVA) separately for each outcome, where *APOE-ε*4 status was entered as a between-subject factor, while age, sex and years of education were modelled as covariates. Since *APOE-ε*4 influences the age-related cognitive decline in healthy

individuals (Caselli et al., 2009, 2011), we further modelled the interaction between *APOE* status and age. Statistical threshold for significance was set to α < 0.05. Structural imaging data were analyzed using Statistical Parametric Mapping software (SPM12, Wellcome Department of Imaging Neuroscience, London, UK). The normalized, modulated and smoothed GM images were entered in a multiple regression design within the general linear model (GLM) implemented in SPM12. To determine the structural brain correlates of EM and EFs in the entire sample, we modelled the effect of each cognitive outcome separately, further controlling for the effects of age, sex, years of education and TIV. To assess the impact of *APOE-ε*4 in modulating the relationship between cognitive performance and regional GMv, we performed a separate GLM, where the variability in cognitive performance was modelled separately for each *APOE-ε*4 subgroup, namely non-carriers (NC), ε4-heterozygous (HE) and ε4-homozygous (HO). This procedure resulted in the inclusion of 3 orthogonal regressors coding the interaction between *APOE* status and cognitive performance. Next, different t-contrasts were performed to test the distinct models of genetic penetrance, namely the dominant, recessive and additive effects, as proposed for the analysis of quantitative trait loci (Clarke et al., 2011). Briefly, an additive model predicts an incremental response of the quantitative trait according to the allelic load, whereas a dominant model predicts a common response to 1 or 2 copies of the risk allele (*i.e.*, ε4-carriers *vs.* non-carriers). Finally, a recessive model predicts a common response to 0 or 1 copy of the risk allele (*i.e.*, non-carriers and ε4-heterozygotes *vs.* ε4-homozygotes). This approach was already implemented in neuroimaging studies investigating the impact of the *APOE* genotype on brain morphology (Cacciaglia et al., 2018a; Filippini et al., 2009). Results were considered significant if surviving a whole-brain voxel-wise statistical threshold of $p < .001$ applying a cluster extent threshold correction of 100 contiguous voxels. This procedure is reliably conservative and further protects against Type I error (Gispert et al., 2015).

Finally, to reduce dimensionality and to search for common patterns of brain morphology associated to EM and EFs, we additionally performed a principal component analysis (PCA) separately for the two cognitive domains and repeated all the above analyses using the extracted principal components as dependent variables (Gaskin and Happell, 2014).

3. Results

3.1. Sample demographic characteristics

Table 1 summarizes the demographic characteristics of our sample. The *APOE* genotype groups did not differ in TIV, male/female ratio, or years of education. There was, however, a significant difference in age with the ε4-homozygous being younger than both non-carriers and ε4-heterozygous. For this reason, age was included as covariate in all subsequent analyses.

3.2. APOE genotype and cognitive performance

Table 2 displays main effects of our independent predictors (*i.e.*,

Table 1
Sample demographic characteristics.

	NC (*N* = 259)	HE (*N* = 204)	HO (N = 64)	Inferential statistics
Age[a] (SD)	57.97 (7.55)	58.23 (7.45)	53.97 (6.07)	$F = 8.85$; $P < .01$
Education[a] (SD)	13.68 (3.62)	13.68 (3.53)	13.44 (3.46)	$F = 0.13$; $P = .88$
TIV[b] (SD)	1448.75 (155.75)	1496.64 (137.84)	1493.82 (136.26)	$F = 0.39$; $P = .67$
Male/female (n)	95/164	93/111	24/40	$\chi^2 = 3.99$; $P = .14$

TIV: Total intracranial volume; NC: Non-Carriers; HE: ε4-heterozygous; HO: ε4-homozygous.
[a] Indicated in years.
[b] Indicated in Cm^3.

Table 2
Cognitive performance in the whole sample assessed for each subtest.

		APOE-ε4 status		Age(y)		APOE x Age		Sex		Education(y)	
		F	P	F	P	F	P	F	P	F	P
Dominant model	TPR	2.99	0.08	11.35	< 0.01	2.41	0.12	4.33	0.04	20.44	< 0.01
	TFR	2.35	0.12	35.77	< 0.01	2.22	0.13	6.01	0.02	12.18	< 0.01
	TDPR	1.81	0.18	11.48	< 0.01	1.35	0.24	4.96	0.03	21.58	< 0.01
	TDFR	0.65	0.42	39.06	< 0.01	0.39	0.53	5.51	0.02	39.06	< 0.01
	SDR	0.01	0.93	3.29	0.07	0.01	0.95	3.47	0.06	10.83	< 0.01
	LDR	0.11	0.73	2.27	0.13	0.16	0.68	6.46	0.01	11.72	< 0.01
	Coding	0.19	0.67	118.7	< 0.01	0.13	0.71	0.94	0.33	67.24	< 0.01
	DSF	0.01	0.97	2.37	0.12	0.02	0.88	25.57	< 0.01	24.80	< 0.01
	DSB	0.86	0.35	6.76	0.01	0.69	0.40	17.04	< 0.01	32.10	< 0.01
	DSS	0.38	0.53	16.74	< 0.01	0.36	0.55	23.31	< 0.01	33.51	< 0.01
	Matrix	0.83	0.36	52.93	< 0.01	0.83	0.36	5.10	0.02	94.25	< 0.01
	Similarities	0.32	0.57	8.25	< 0.01	0.23	0.62	8.97	< 0.01	126.4	< 0.01
	VP	0.33	0.56	40.31	< 0.01	0.26	0.61	47.88	< 0.01	43.70	< 0.01
Recessive model	TPR	0.99	0.32	0.56	0.45	1.39	0.23	3.87	0.05	20.25	< 0.01
	TFR	0.01	0.94	9.05	< 0.01	0.04	0.84	5.74	0.01	12.23	< 0.01
	TDPR	1.14	0.28	0.52	0.46	1.54	0.21	4.52	0.03	21.42	< 0.01
	TDFR	0.01	0.94	9.98	< 0.01	0.04	0.83	5.00	0.02	17.07	< 0.01
	SDR	2.71	0.10	0.04	0.82	2.47	0.11	3.48	0.06	10.34	< 0.01
	LDR	0.62	0.43	0.20	0.65	0.40	0.52	6.48	0.01	11.18	< 0.01
	Coding	0.86	0.35	26.01	< 0.01	0.98	0.32	1.10	0.29	67.64	< 0.01
	DSF	1.81	0.17	0.18	0.67	2.13	0.14	26.43	< 0.01	24.68	< 0.01
	DSB	0.15	0.69	0.66	0.41	0.33	0.56	17.77	< 0.01	32.49	< 0.01
	DSS	0.10	0.74	4.85	0.03	0.02	0.89	23.89	< 0.01	34.37	< 0.01
	Matrix	0.02	0.88	16.07	< 0.10	0.01	0.93	5.06	0.02	94.80	< 0.01
	Similarities	0.37	0.54	1.21	0.27	0.36	0.54	9.27	< 0.01	125.2	< 0.01
	VP	0.13	0.71	13.16	< 0.01	0.08	0.77	47.57	< 0.01	44.49	< 0.01
Additive model	TPR	2.44	0.08	2.75	0.08	2.43	0.08	4.54	0.03	20.50	< 0.01
	TFR	1.06	0.34	17.67	< 0.01	1.09	0.33	5.94	0.01	12.28	< 0.01
	TDPR	1.87	0.15	2.54	0.10	1.88	0.15	5.09	0.02	21.63	< 0.01
	TDFR	0.26	0.77	19.01	< 0.01	0.20	0.81	5.42	0.02	17.14	< 0.01
	SDR	1.71	0.18	0.21	0.64	1.50	0.22	3.86	0.05	10.41	< 0.01
	LDR	0.34	0.71	0.80	0.37	0.21	0.80	6.89	< 0.01	11.23	< 0.01
	Coding	0.47	0.62	52.09	< 0.01	0.50	0.61	0.94	0.33	67.32	< 0.01
	DSF	0.98	0.37	0.01	0.91	1.11	0.33	25.21	< 0.01	24.75	< 0.01
	DSB	0.43	0.64	1.94	0.16	0.50	0.60	17.16	< 0.01	32.47	< 0.01
	DSS	0.08	0.92	8.36	< 0.01	0.05	0.95	23.86	< 0.01	34.22	< 0.01
	Matrix	0.64	0.52	27.42	< 0.01	0.61	0.54	5.26	0.02	94.53	< 0.01
	Similarities	0.57	0.56	3.21	0.07	0.49	0.61	8.65	< 0.01	125.2	< 0.01
	VP	0.51	0.59	21.67	< 0.01	0.39	0.67	48.57	< 0.01	44.28	< 0.01

TPR: Total paired recall; TFR: Total free recall; TDPR: Total delayed paired recall; TDFR: Total delayed free recall; SDR: Short-delay retention; LDR: Long-delay retention; DSF: Digit-span forward; DSB: Digit-span backwards; DSS: Digit-span sequence; VP: Visual Puzzles.

APOE-ε4, age, sex, and years of education) as well as the interaction between APOE-ε4 and age on cognitive performance in EM and EFs. None of the three genotypic models yielded significant main effects of APOE-ε4 on EM or EFs performance. Irrespective of the genetic model of penetrance, immediate as well as delayed recall performance significantly declined with increasing age, however both short- and long-delay retention did not show an age-related decline (Table 2; Supplementary Fig. 3). All measures of EFs showed a significant age-related effect except the digit-span forward and digit-span backward (Table 2). Additionally, while female subjects performed better in recall performance, males obtained significantly higher scores in EFs (Table 2; Supplementary Fig. 3). A confirmatory analysis performed on the first principal component for each cognitive domain yielded similar results (Supplementary Table 1).

3.3. Impact of APOE-ε4 on the associations between EM performance and GMv

Supplementary Table 2 displays the brain volumetric correlates of cognitive performance in the whole sample, which are in line with our previous study conducted on a subsample of the present one (Cacciaglia et al., 2018b). We detected significant interactions between EM performance and APOE status in all the MBT outcomes, indicating that APOE-ε4 significantly modified the relationships between EM

proficiency and gray matter morphology (Table 3). Figs. 1 and 2 display these effects in selected brain regions separately for paired and free recall. The dominant, recessive and additive models mapped onto shared brain areas, such as the inferior temporal gyrus, the dorsal anterior cingulate cortex as well as the cuneus for the TFR, and the basal forebrain cholinergic nuclei for the TDPR. For TDFR, the recessive and the additive models shared several regions including the inferior superior temporal cortex, the precuneus and the posterior cingulate gyrus. The shared topology among different genotypic contrasts in some areas does not assure that variability in that specific region is equally summarized by those contrasts. To provide statistical evidence of this, we performed a conjunction analysis in SPM asking for all common brain regions in pairs of t-contrasts (i.e., dominant-recessive, dominant-additive, recessive-additive). Results show that for most cognitive outcomes, there are no shared brain regions between the dominant and the recessive models (Supplementary Table 3). Table 4 and Fig. 3 illustrate significant interaction effects for short as well as long-delay retention index (SDR, LDR). In both retention indices, there were no shared brain regions between the dominant and the recessive models, suggesting that these two genotypic models captured distinct biological mechanisms. For SDR, the dominant and the additive models revealed significant interactions in the right and left hippocampus as well as the bilateral insula and the posterior cingulate, with these effects additionally surviving correction for multiple testing on the cluster level

Table 3
APOE-ε4 significantly modulated the relationship between EM performance and regional GMv.

	Brain region	Laterality	*t*-value*	k**	MNI coordinates		
					x	y	z
Episodic Memory							
TPR							
ε4-dominant	Middle frontal	R	4.55	135	33	29	33
	Dorsal anterior cingulate	L	4.46	290	−9	27	36
	Insula[a]	L	4.29	618	−35	−14	14
	Precuneus	L	4.00	316	0	−56	32
	Insula	R	4.00	299	41	−11	11
	Basal forebrain	R	3.97	103	15	−3	−12
	Frontal operculum	R	3.96	105	41	15	12
	Basal forebrain	L	3.86	365	−9	3	−15
ε4-recessive	Posterior cingulate	L	3.71	127	0	−41	24
ε4-additive	Middle frontal	R	4.61	104	33	29	33
	Insula	L	4.14	249	−38	−11	9
	Dorsal anterior cingulate	R	4.12	182	−9	29	36
	Posterior cingulate	L	3.89	295	0	−41	24
	Orbitofrontal gyrus	L	3.82	100	−9	51	−29
	Basal forebrain	L	3.63	236	−11	3	−17
TFR							
ε4-dominant	Dorsal anterior cingulate	L	4.56	278	−9	27	35
	Cuneus	R	4.34	204	20	−71	21
	Inferior Temporal	L	4.27	270	−54	−39	−17
	Superior temporal	L	4.23	304	−39	−17	−3
	Insula	R	4.14	415	39	−11	9
	Insula[a]	L	4.02	479	−36	−2	9
	Precuneus	R	3.98	207	9	−45	17
	Angular gyrus	R	3.84	126	29	−56	42
	Rectus	L	3.84	113	−6	17	−24
	Basal forebrain	L	3.73	136	−11	5	−12
	Rectus	L	3.63	222	−6	45	−20
ε4-recessive	Inferior temporal	R	4.88	227	57	−44	−14
	SMA	R	4.43	353	5	12	56
	Cuneus	R	4.12	136	18	−74	24
	Middle cingulate	L	3.86	228	−8	−3	36
	Precuneus[a]	L	3.80	496	−3	−62	29
	Paracentral lobule	L	3.75	158	−8	−26	57
	Dorsal anterior cingulate	L	3.63	125	−9	27	35
	Precuneus	L	3.57	104	−11	−48	11
	Cerebellum lob. 6	R	3.44	141	30	−63	−21
ε4-additive	Inferior temporal	R	4.74	219	57	−45	−12
	Cuneus	R	4.53	207	20	−72	23
	Dorsal anterior cingulate[a]	L	4.39	529	−9	27	35
	Inferior temporal	L	4.12	120	−53	−39	−17
	SMA	R	4.10	292	3	11	57
	Middle occipital gyrus	L	4.08	112	−47	−78	−2
	Posterior cingulate[a]	L	4.01	1063	0	−54	30
	Insula	L	3.88	212	−36	−20	−5
	Entorhinal cortex	R	3.85	130	23	−2	−36
	Basal forebrain	L	3.66	100	−11	3	−17
TDPR							
ε4-dominant	Dorsal anterior cingulate	L	4.38	329	−9	27	36
	Precuneus	L	4.16	135	0	−56	32
	Middle fontal gyrus	R	4.15	104	33	29	33
	Rolandic operculum	L	4.14	442	−39	−9	9
	Insula	R	4.00	204	39	−11	9
	Frontal operculum	R	3.98	199	41	15	12
	Basal forebrain[a]	L	3.95	480	−11	3	−17
	Fusiform gyrus	L	3.66	190	−35	−11	−41
ε4-recessive	SMA	R	4.49	167	5	12	54
	Frontal operculum	R	3.86	107	42	14	11
	Dorsal anterior cingulate	L	3.66	110	−9	29	36
	Basal forebrain	L	3.38	123	−3	14	−15
ε4-additive	SMA	R	4.37	170	6	12	54
	Frontal operculum	R	4.20	166	41	15	12
	Dorsal anterior cingulate	L	4.20	316	−9	27	36
	Insula	L	4.00	172	−38	−11	11
	Basal forebrain[a]	L	4.00	523	−11	3	−17
	Insula	R	3.91	103	41	−11	9
TDFR							

Table 3 (*continued*)

	Brain region	Laterality	t-value[*]	k[**]	MNI coordinates		
					x	y	z
ε4-dominant	Basal forebrain	L	4.20	288	−11	3	−15
	Insula	R	4.08	446	38	−12	−3
	Caudate nucleus	R	4.02	358	3	6	2
	Insula	L	3.95	106	−32	−3	15
	Superior temporal[a]	L	3.94	486	−39	−17	−3
ε4-recessive	Inferior temporal[a]	R	4.77	173	57	−44	−14
	SMA	R	4.28	300	6	12	56
	Dorsal anterior cingulate	R	3.89	130	0	32	32
	Precuneus	L	3.82	122	−3	−63	30
	Posterior cingulate	R	3.60	272	9	−38	30
	Precuneus	R	3.58	172	12	−47	11
ε4-additive	Inferior temporal	R	4.24	109	57	−45	−12
	Dorsal anterior cingulate	L	4.11	179	0	32	32
	SMA	R	4.05	262	8	12	54
	Basal forebrain	L	3.96	193	−11	3	−17
	Precuneus	L	3.94	223	−3	−63	30
	Insula	L	3.79	172	−36	−20	−5
	Posterior cingulate	R	3.33	107	8	−44	24

MNI: Montreal Neurological Institute; TPR: Total paired recall; TFR: Total free recall; TDPR: Total delayed paired recall; TDFR: Total delayed free recall; SMA: Supplementary motor area.

[*] Significant at a whole-brain threshold of p < .001, with a cluster size correction of 100 contiguous voxels.

[**] Cluster size indicated in number of contiguous voxels.

[a] Additionally survived correction for multiple testing on the cluster level (p < .05) computed with a Family-Wise Error rate approach (FWE).
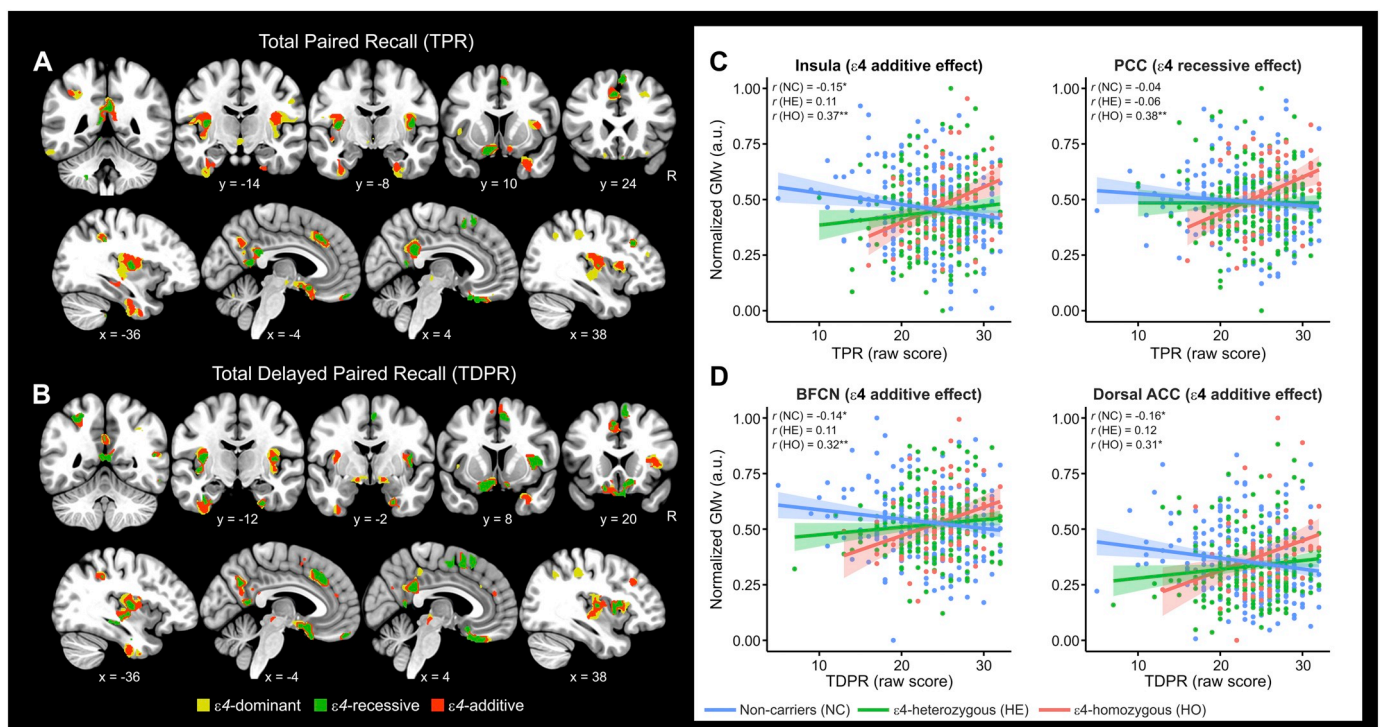

Fig. 1. *APOE-ε4 risk variant modulated the associations between paired recall and gray matter volume.*
A) and B) Voxel-wise volumetric maps showing the dominant, recessive and additive effects of *APOE-ε4* in modulating the association between immediate as well as delayed paired recall (TPR, TDPR) and gray matter structure For visualization purposes parametric maps are thresholded at $p < .005$ with a cluster extent threshold of 100 voxels. C) and D) Group scatterplots in selected brain regions showing the significant interactions between immediate as well as delayed paired recall performance (TPR, TDPR) and *APOE-ε4* status. Values of gray matter volume were extracted on the voxel level (cluster's local maximum) and adjusted for the covariates in the model (*i.e.*, age, sex, years of education and total intracranial volume). Pearson's correlation coefficients are shown on top of scatterplots for each subgroup. *$p < .05$, **$p < .01$, two-tailed. Shaded areas indicate 90% confidence intervals. ACC: Anterior cingulate cortex; BFCN: Basal forebrain cholinergic nuclei; PCC: Posterior cingulate cortex.

(using a family-wise error rate [FWE] approach). For LDR, the dominant model yielded significant effects in the middle and posterior cingulate cortex as well as the bilateral insula and the inferior parietal cortex. By contrast, the recessive model mapped onto different regions, such as the entorhinal cortex as well as the superior frontal cortex and the cerebellum (lobule 8). In all brain regions *APOE-ε4* carriership shifted the association between EM performance and regional GMv from being negative to positive (Figs. 1–3).
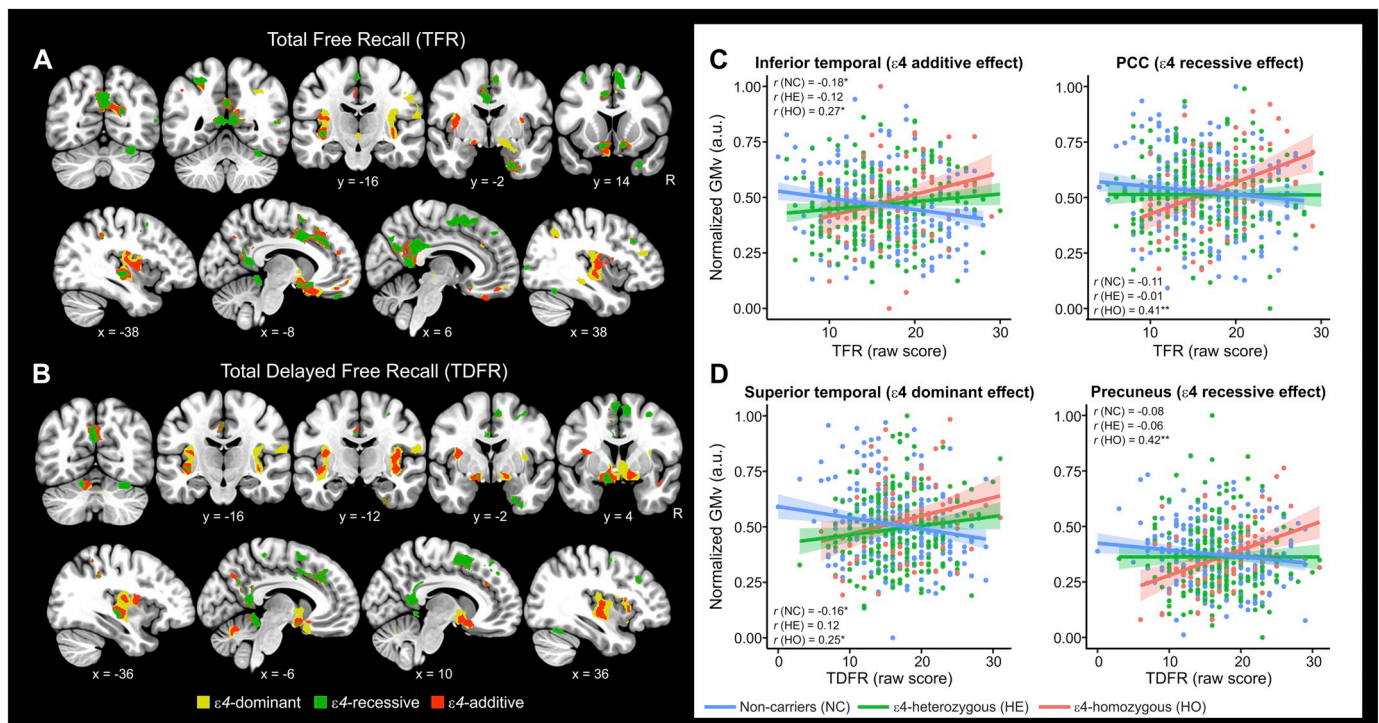
Fig. 2. *APOE-ε*4 risk variant modulated the associations between free recall and gray matter volume.
A) and B) Voxel-wise volumetric maps showing the dominant, recessive and additive effects of *APOE-ε*4 in modulating the association between delayed free recall (TFR, TDFR) and gray matter structure. For visualization purposes parametric maps are thresholded at p < .005 with a cluster extent threshold of 100 voxels. C) and D) Group scatterplots in selected brain regions showing the significant interactions between immediate as well as delayed paired recall performance (TFR, TDFR) and *APOE-ε*4 status. Values of gray matter volume were extracted on the voxel level (cluster's local maximum) and adjusted for the covariates in the model (*i.e.*, age, sex, years of education and total intracranial volume). Pearson's correlation coefficients are shown on top of scatterplots for each subgroup. *p < .05, **p < .01, two-tailed. Shaded areas indicate 90% confidence intervals. PCC: Posterior cingulate cortex.

3.4. Impact of APOE-ε4 on the associations between EFs performance and GMv

APOE-ε4 modulated the association between GMv and efficiency in EFs. Of the administered tests, we detected significant interactions for the Coding, digit-span sequencing and the Visual Puzzles (Table 5). Fig. 4 displays these effects in selected brain regions. For the Coding test, the three genotypic models yielded significant effects in a set of common brain regions including the lateral as well as medial orbito-frontal cortex and the precentral gyrus. For the digit-span sequencing, we observed significant effects in the caudate nucleus (both recessive and additive models) and the middle orbital gyrus (recessive model). Finally, for the VP, significant interaction effects were observed in the postcentral gyrus (both recessive and additive models) and the superior frontal cortex (additive model).

The direction of these interaction effects was opposite compared to that observed for EM (*i.e.*, *APOE*-ε4 shifted the relationships from being positive to negative). A confirmatory analysis performed on the first principal component for both EM and EFs yielded similar results (Supplementary Table 4).

4. Discussion

We report that the *APOE* genotype modifies the association between cognitive performance and the underlying cerebral morphology as expressed by regional GMv, in cognitively healthy individuals. In both domains of EM and EFs, *APOE*-ε4 carriers displayed reversed relationships between regional brain volumes and cognitive performance in a highly symmetrical topological pattern. More specifically, presence of *APOE*-ε4 shifted the associations between EM and regional GMv from negative to positive, while driving the opposite effect on the

relationship with EFs. These effects resemble those observed in our previous study, where we reported a qualitatively similar modulatory role for aging in modifying the structure-function relationship (Cacciaglia et al., 2018b). In our earlier report, we found that older age shifted the association between GMv and EM performance from being negative to positive, corroborating findings by other research groups (Van Petten, 2004).We proposed that, while for younger individuals reduced brain volumes in dedicated brain areas may be the result of successful neurodevelopmental events which increase efficiency (*e.g.*, synaptic pruning), larger GMv in advanced age would represent a proxy for available brain reserve, therefore supporting memory performance. Following this postulate, the results of the present study suggest that *APOE*-ε4 carriers display a pattern of structure-function association corresponding to an older age than their chronological one. If so, our data would provide a biological underpinning for the hypothesis that *APOE*-ε4 confers an accelerated aging process in the brain (Cacciaglia et al., 2018a; Evans et al., 2014; Filippini et al., 2011). In line with this, longitudinal studies reported a faster age-related decline of episodic memory in unimpaired *APOE*-ε4 carriers, with a gene-dose dependent effect (Caselli et al., 2009). Alternatively, our interaction data may be indicative of age-independent neurodevelopmental effects of the ε4 allele on the brain morphology (Dean 3rd et al., 2014; Chang et al., 2016), which may lead to a distinctive cerebral organization supporting cognitive functioning during the entire lifespan. Additionally, it may be that a proportion of our ε4-homozygous individuals have already entered the preclinical stage of AD, with the pathology possibly affecting the structural network underlying cognition. This latter consideration remains however uncertain given the lack of core AD biomarkers in the current study.

The dissociation we found between cerebral volumes and performance in EM *vs.* EFs resembles that of our former study conducted in a

Table 4
APOE-ε4 significantly modulated the relationship between delayed retention and regional GMv.

	Brain region	Laterality	t-value[*]	k[**]	MNI coordinates		
					x	y	z
Short-delay retention							
ε4-dominant	Insula[a]	L	5.05	982	−35	−24	0
	Insula[a]	R	4.90	1261	42	−20	−6
	Middle temporal	L	4.71	135	−42	−69	11
	Inferior frontal	R	4.41	220	38	41	18
	Hippocampus[a]	R	4.29	732	14	−6	−24
	Posterior cingulate[a]	L	4.28	458	−6	−47	26
	Hippocampus[a]	L	4.05	908	−24	−14	−20
	Inferior parietal	L	4.00	118	−27	−54	54
ε4-recessive	Entorhinal cortex	R	4.10	129	24	−14	−36
ε4-additive	Inferior frontal	R	4.21	193	39	39	20
	Entorhinal cortex	R	4.09	323	24	−14	−36
	Insula	L	4.05	245	−36	−26	0
	Insula[a]	R	3.89	570	35	−23	2
	Cerebellum Lob. 8	L	3.84	155	−35	−39	−45
	Posterior cingulate	L	3.69	119	−9	−48	14
	Hippocampus	L	3.63	126	−23	−14	−20
Long-delay retention							
ε4-dominant	Middle cingulate[a]	R	4.51	563	0	−39	41
	Inferior parietal	L	4.39	359	−26	−53	56
	Insula	R	4.04	104	42	−20	−6
	Posterior cingulate	R	4.04	139	0	−56	30
	Insula	R	3.73	290	32	−27	17
	Insula	L	3.59	182	−36	−14	14
ε4-recessive	Entorhinal cortex	R	4.51	201	26	−14	−36
	Superior frontal	R	3.97	181	9	8	54
	Cerebellum Lob. 8	L	3.97	123	−33	−39	−45
ε4-additive	Entorhinal cortex	R	4.60	206	26	−14	−36
	Cerebellum Lob. 8	L	4.12	186	−33	−39	−45
	Superior frontal	R	4.10	217	9	8	56
	Posterior cingulate	R	3.91	197	0	−56	30
	Insula	R	3.57	116	32	−27	17

[*] Significant at a whole-brain threshold of $p < .001$. with a cluster size correction of 100 contiguous voxels.
[**] Cluster size indicated in number of contiguous voxels.
[a] Additionally survived correction for multiple testing on the cluster level ($p < .05$) computed with a Family-Wise Error rate approach (FWE).

subsample of the present one, where we observed negative relationships for EM but positive correlations for EFs (Cacciaglia et al., 2018b). This divergence is reconciled if one considers that the brain structures supporting EM (*i.e.*, medial temporal lobe) and EFs (prefrontal cortex) display different time-course maturation patterns, with medial temporal lobe rapidly evolving during childhood, while prefrontal areas reaching complete maturation only in the adulthood (Ghetti and Bunge, 2012). Therefore, compared to prefrontal areas, medial temporal lobe regions may be more subject to neurodevelopmental events such as synaptic pruning, which optimize neural computational efficiency (Tau and Peterson, 2010). Besides, the observed dissociation on the brain structure level, was already reported in functional MRI studies which have observed deactivation in "task-negative" networks during successful encoding (Kim et al., 2010), while observing an increase of activation in the executive control network supporting EFs (Murphy et al., 2018).

In the analysis of EM, we found that the three genotypic models mapped onto common brain regions, such as the dorsal anterior cingulate and the inferior temporal gyrus. However, for TPR and TDFR there were no shared brain regions between the dominant and the recessive models. The same was true for SDR and LDR, indicating that these two models were associated to distinct brain structural imaging phenotypes. Across all the MBT outcomes, the additive model, which assumes an increased genetic penetrance according to the number of risk alleles, yielded significant effects in the right and left basal forebrain cholinergic nuclei (BFCN) (Zaborszky et al., 2008). These consist of four nuclei which provide the major cholinergic source to the hippocampus and prefrontal areas (Mesulam, 2004). Cholinergic signaling in the CNS ensures cortical activation, promotes vigilance, and supports

cognitive effort during attentional tasks (Ballinger et al., 2016). Importantly, BFCN undergo progressive degeneration during the course of AD (Teipel et al., 2005) and previous studies detected BCFN atrophy prior to the onset of cognitive symptoms in healthy individuals who later converted to AD (Schmitz et al., 2016; Grothe et al., 2013; Hall et al., 2008). Additionally, Hanyu et al. (2002) reported that the thickness of the BFCN positively correlated with global cognition in AD, but not in other forms of dementia, suggesting that cognitive dysfunction in AD is at least partially attributable to cholinergic dysfunction. Similarly, George et al. (2011) reported significantly positive associations in mild cognitive impairment (MCI) and AD patients, between BFCN volume and immediate as well as delayed recall assessed using a similar memory paradigm as ours. Hence our results suggest that, unlike in non-carriers, EM efficiency in individuals at higher genetic risk for AD depends on the integrity of brain structures which overlap with those in AD patients, although being within normal ranges. Importantly, an abnormal pattern of age-related BCFN structural degeneration has been shown to parallel Aβ positivity in cognitively healthy people (Schmitz et al., 2018). Thus, it may be that among our healthy ε4-homozygous, those having lower BFCN volumes and consequently worse EM, may display Aβ deposition and have already entered a preclinical stage of AD. However, the lack of biomarker data in our study prevents us to draw such a conclusion.

Other brain regions that were identified by the additive model across the four recall outcomes of the MBT were the bilateral insula and the dorsal anterior cingulate cortex, both central nodes of the previously described salience network (Seeley et al., 2007). The insula displays reciprocal connections with the BFCN (Zaborszky et al., 2015), and prior studies have highlighted its involvement in performance
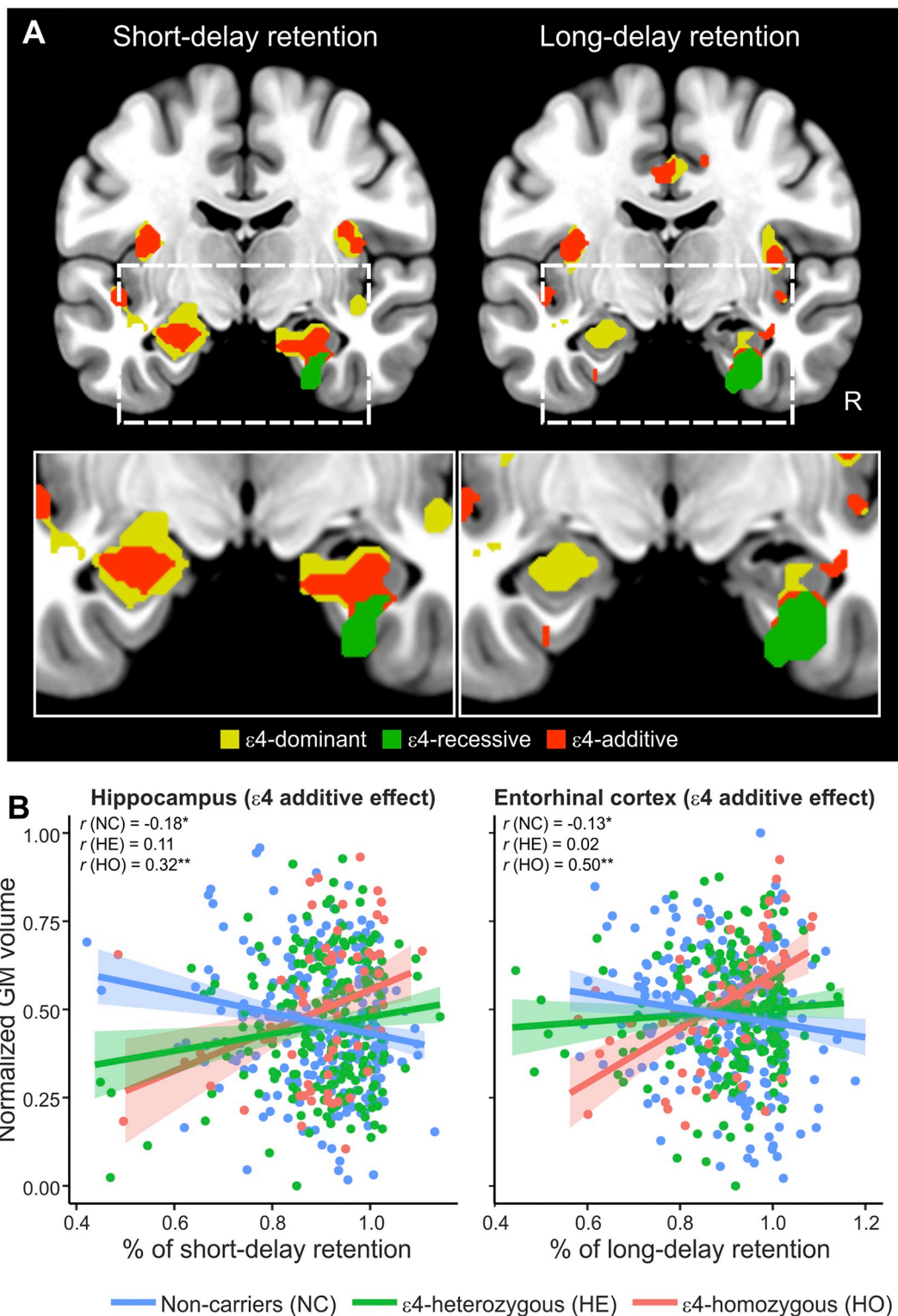
Fig. 3. Effects of the *APOE-ε4* risk variant in modifying the association between memory retention and regional gray matter volume.
A) Dominant, recessive and additive effects of *APOE-ε4* in modulating the association between short- and long-delay retention (SDR, LDR) and regional gray matter volume. Significant clusters are projected over coronal slices. B) Group scatterplots in selected brain regions showing the significant interactions between SDR as well as LDR and *APOE-ε4* status in the gray matter volume of hippocampus and entorhinal cortex, respectively. Values of gray matter volume were extracted on the voxel level (cluster's local maximum) and adjusted for the covariates in the model (*i.e.*, age, sex, years of education and total intracranial volume). Pearson's correlation coefficients are shown on top of scatterplots for each subgroup. *p < .05, **p < .01, two-tailed. Shaded areas indicate 90% confidence intervals.

monitoring (Cosentino et al., 2015) and error awareness (Klein et al., 2007). In this framework, our findings suggest that *APOE-ε4* carriers rely on the integrity of multiple compensatory brain systems in order to achieve an equivalent memory performance to non-carriers, possibly

due to an incipient degeneration of brain areas supporting cognitive performance (Cacciaglia et al., 2018a; Operto et al., 2018).In line with this, previous functional MRI studies have consistently show that early-middle age cognitively healthy *APOE-ε4* carriers display

Table 5
APOE-ε4 significantly modulated the relationship between EFs performance and regional GMv.

	Brain region	Laterality	t-value[*]	k[**]	MNI coordinates		
Executive function							
Coding							
ε4-dominant	Lateral orbitofrontal[a]	R	4.84	530	39	45	−12
	Precentral gyrus	L	4.50	193	−39	−6	48
	Superior orbitofrontal	R	3.85	148	21	38	−15
	Medial orbitofrontal	L	3.78	101	−21	6	−17
ε4-recessive	Medial orbitofrontal[a]	L	5.58	1980	−21	6	−17
	Lateral orbitofrontal[a]	R	5.13	1393	41	44	−11
	Precentral gyrus[a]	L	4.78	357	−41	−6	48
	Lateral orbitofrontal[a]	L	4.45	548	−42	51	−5
	Anterior cingulate	L	3.95	257	−12	42	2
	Middle cingulate	R	3.95	200	8	−30	42
	Rectal gyrus	R	3.63	212	6	35	−14
ε4-additive	Lateral orbitofrontal [a]	R	5.36	1339	39	45	−12
	Medial orbitofrontal[a]	L	5.24	870	−21	6	−17
	Precentral gyrus[a]	L	5.01	324	−39	−6	48
	Lateral orbitofrontal	L	4.46	441	−44	51	−5
	Medial orbitofrontal[a]	R	4.35	459	21	6	−18
DSS							
ε4-recessive	Middle orbital gyrus	L	4.08	380	−15	54	−14
	Caudate nucleus	L	3.74	202	−12	8	18
ε4-additive	Caudate nucleus	L	3.89	279	−14	8	18
	Caudate nucleus	R	3.53	168	12	11	17
VP							
ε4-recessive	Postcentral gyrus[a]	L	4.80	620	−27	−44	54
ε4-additive	Postcentral gyrus[a]	L	4.38	451	−27	−44	56
	Superior frontal	L	3.86	180	−17	56	21

MNI: Montreal Neurological Institute; DSS: Digit-span sequencing; VP: Visual puzzles.

[*] Significant at a whole-brain threshold of p < .001, with a cluster size correction of 100 contiguous voxels.

[**] Cluster size indicated in number of contiguous voxels.

[a] Additionally survived correction for multiple testing on the cluster level (p < .05) computed with a Family-Wise Error rate approach (FWE).

hyperactivation in temporal and frontal areas during episodic as well as working memory tasks (Filippini et al., 2011; Bondi et al., 2005; Bookheimer et al., 2000; Wishart et al., 2006) which has been interpreted as signature of neural compensation (see Han and Bondi, 2008 for a review). This view is further corroborated by previous studies which have proposed the BFCN as a substrate for neuronal adaptation. With this respect, Croxson et al. (2012) found that cholinergic input to temporal regions facilitates the recovery of function after structural damage to the circuitry mediating episodic memory. Ray et al. (2015) showed that patients with MCI present a shift from fornix- to para-hippocampal-based circuitry in order to preserve their residual memory, and that this reallocation was dependent on the volume of the BFCN. The recessive model yielded significant interaction effects predominantly in midline cortical areas spanning from the dorsal anterior (TFR, TDPR) to the posterior cingulate gyrus (TPR), including the precuneus (TFR). For measures of immediate and delayed free recall, the recessive model also returned significant interactions in the inferior temporal regions. All these regions are subject to early accumulation of fibrillary Aβ in healthy *APOE-ε*4 carriers (Rodrigue et al., 2012) with these effects being highest in ε4-homozygous (Reiman et al., 2009). Additionally, lower glucose metabolism in the precuneus and posterior cingulate cortex has been observed in relation to the number of ε4 alleles in cognitively intact individuals (Protas et al., 2013; Reiman et al., 2005). Thus, our recessive model seems pointing to areas that are specifically vulnerable to Aβ deposition. Notably, cognitively intact subjects with cerebral Aβ burden in midline cortical areas display over-activation in task-positive networks during recall and this hyperactivity correlates with recall precision, indicating a mechanism of neural compensation (Elman et al., 2014). It is therefore plausible that a similar mechanism is operating in our ε4-homozygous subjects given the close association between *APOE-ε*4 homozygosity and brain amyloidosis. In fact, at the mean age in our sample, about 50% of ε4-homozygous are expected to harbor Aβ pathology (Jansen et al., 2015).

In addition to immediate and delayed recall, we computed the percentage of retained words after short and long delay with respect to the number of encoded items. Delayed retention provides different information compared to recall, because it is controlled for potential encoding-related effects and it is relatively unaffected by aging (Brickman et al., 2011). We could confirm that, unlike recall outcomes, both SDR and LDR were unaffected by advancing age (Supplementary Fig. 3). Earlier studies have shown that deficient delayed retention predicts the onset of dementia years before (Lange et al., 2002; Elias et al., 2000). We did not observe a significant impact of *APOE-ε*4 on delayed retention performance, however we did observe interaction effects similar to that described for recall measures, although with a partially different topology. For SDR the interaction involved the head of hippocampus bilaterally, which additionally survived FWE correction on the cluster level. For LDR we observed a significant interaction in the right entorhinal cortex. The specificity of delayed retention measures may have engaged a compensatory strategy in these areas. Yet, other mechanisms apart from compensation may underlie these interactions, since SDR and LDR were the only two outcomes of EM where the homozygote group tended to perform worse than the rest, possibly indicating an incipient failure of compensatory strategies for this specific facet of EM (Supplementary Fig. 1).

We next examined EFs and found that *APOE-ε*4 shifted the association between GMv and performance on cognitive processing speed (CPS, assessed with the Coding test) as well as working memory (assessed through the digit-span sequencing) from being positive to negative, again mirroring our previous data on the interaction between executive functions and aging (Cacciaglia et al., 2018b). Effects for CPS included orbitofrontal, prefrontal and middle cingulate cortex across the three genotypic models, although the strongest significance values were observed in the recessive and additive models where several regions survived FWE correction. CPS efficiency depends on the integrity of white matter fibers (Borghesani et al., 2013; Kochunov et al., 2010) and we have recently shown white matter microstructural degeneration in the homozygote group of the present sample (Operto et al., 2018). It
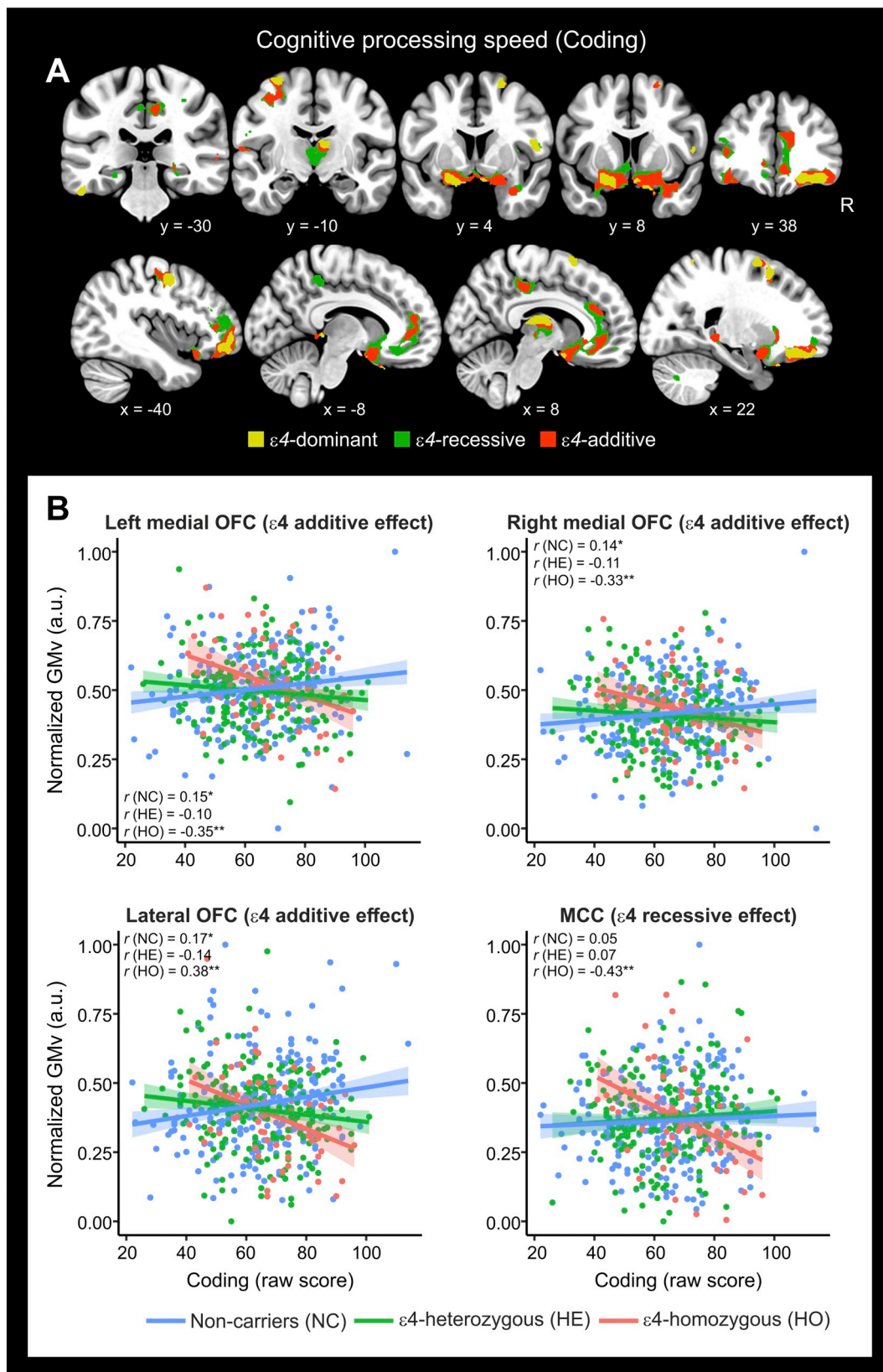
Fig. 4. *APOE-ε4* risk variant modulated the associations between cognitive processing speed (CPS) and gray matter volume.
A) Dominant, recessive and additive effects of *APOE-ε4* in modulating the association between short- and long-delay retention (SDR, LDR) and regional gray matter volume. Significant clusters are projected over coronal slices. For visualization purposes parametric maps are thresholded at p < .005 with a cluster extent threshold of 100 voxels. B) Group scatterplots in selected brain regions showing the significant interactions between CPS performance and *APOE-ε4* status. Values of gray matter volume were extracted on the voxel level (cluster's local maximum) and adjusted for the covariates in the model (*i.e.*, age, sex, years of education and total intracranial volume). Pearson's correlation coefficients are shown on top of scatterplots for each subgroup. *p < .05, **p < .01, two-tailed. Shaded areas indicate 90% confidence intervals. OFC: Orbitofrontal cortex; MCC: Middle cingulate gyrus.

is possible that, due to inefficient recruitment of white matter circuitry, reduced GMv in orbitofrontal areas aids processing speed in *APOE-ε4* homozygous. For example, the orbitofrontal cortex is considered a critical region for motor response inhibition (Bryden and Roesch, 2015; Rodrigo et al., 2014), hence less volume in these areas would facilitate or sustain motor activation necessary for this task. Accordingly, a reduced volume in the middle cingulate gyrus would disengage conflict monitoring, supporting the execution of the psychomotor task (Parvaz et al., 2014; Sohn et al., 2007). In support of this, increased thickness in frontal areas in healthy *APOE-ε4* carriers predicted worse performance in attentional tasks (Espeseth et al., 2012). Alternatively, larger volume in prefrontal and orbitofrontal areas in *APOE-ε4* homozygotes may be the result of incipient neuroinflamatory processes exacerbated by the ε4 allele (Wolf et al., 2013), which in turn interferes with efficient executive functions.

Finally, we did not detect a significant impact of *APOE-ε4* allele load on either memory or executive functions, in line with the lack of consistent findings in the literature on the effect of this risk variant on cognitive performance (O'Donoghue et al., 2018). Genetic epistasis as well as additional environmental factors may moderate the direct impact of *APOE* status on cognition and future research shall take these variables into consideration. As mentioned above, the lack of core AD biomarkers represents a limitation of the present study. The inclusion of these data would allow to disentangle whether the observed effects are further moderated by amyloid or tau positivity. Another limitation is represented by the cross-sectional nature of our study design. Since *APOE-ε4* has been suggested to impact cognition differentially across life stages (*i.e.*, the antagonistic pleiotropy hypothesis, reviewed in Tuminello and Han, 2011), longitudinal follow-up is required to delineate the lifetime trajectories of the interaction effects between cognition and *APOE* status.

In summary, our study provides novel insights on the mechanisms through which *APOE-ε4* posits an increased risk for AD, by showing that presence of this risk allele modulates the association between cognitive function and the underlying gray matter morphology. Even though the assessed genotypic models revealed overlapping results, several brain regions were model-specific. However, the additive model was the one that better summarized the impact of the risk variant on our neuroimaging outcomes, as it captured a cerebral topology in conjunction with either the dominant or the recessive ones. This lends further support to the previously reported dose-dependent risk for AD exerted by the *APOE-ε4* allele (Corder et al., 1993; Farrer et al., 1997). Finally, our data suggest that cognitive efficiency may undergo continuous compensation during healthy aging and in individuals at risk for dementia, making difficult to bridge the gap between genes and cognition without considering the underlying biological endophenotype. Future research shall address what factors moderate successful neural compensatory strategies and when this starts to eventually lead to neurodegeneration.

Acknowledgemnts

Appendix A. Supplementary data

Supplementary data to this article can be found online at https://doi.org/10.1016/j.nicl.2019.101818.

References

Alexander, G.E., Bergfield, K.L., Chen, K., Reiman, E.M., Hanson, K.D., Lin, L., Bandy, D., Caselli, R.J., Moeller, J.R., 2012. Gray matter network associated with risk for Alzheimer's disease in young to middle-aged adults. Neurobiol. Aging 33, 2723–2732.

Ashburner, J., 2007. A fast diffeomorphic image registration algorithm. Neuroimage 38, 95–113.

Ballinger, E.C., Ananth, M., Talmage, D.A., Role, L.W., 2016. Basal forebrain cholinergic circuits and Signaling in cognition and cognitive decline. Neuron 91, 1199–1218.

Bondi, M.W., Houston, W.S., Eyler, L.T., Brown, G.G., 2005. fMRI evidence of compensatory mechanisms in older adults at genetic risk for Alzheimer disease. Neurology 64, 501–508.

Bookheimer, S.Y., Strojwas, M.H., Cohen, M.S., Saunders, A.M., Pericak-Vance, M.A., Mazziotta, J.C., Small, G.W., 2000. Patterns of brain activation in people at risk for Alzheimer's disease. N. Engl. J. Med. 343, 450–456.

Borghesani, P.R., Madhyastha, T.M., Aylward, E.H., Reiter, M.A., Swarny, B.R., Schaie, K.W., Willis, S.L., 2013. The association between higher order abilities, processing speed, and age are variably mediated by white matter integrity during typical aging. Neuropsychologia 51, 1435–1444.

Brickman, A.M., Stern, Y., Small, S.A., 2011. Hippocampal subregions differentially associate with standardized memory tests. Hippocampus 21, 923–928.

Bryden, D.W., Roesch, M.R., 2015. Executive control signals in orbitofrontal cortex during response inhibition. J. Neurosci. 35, 3903–3914.

Bunce, D., Bielak, A.A., Anstey, K.J., Cherbuin, N., Batterham, P.J., Easteal, S., 2014. APOE genotype and cognitive change in young, middle-aged, and older adults living in the community. J. Gerontol. A Biol. Sci. Med. Sci. 69, 379–386.

Buschke, H., 2014. Rationale of the memory binding test. In: Nilsson, L., Ohta, N. (Eds.), Dementia and Memory. Psychology Press, Hove, East Sussex, pp. 55–71.

Cacciaglia, R., Molinuevo, J.L., Sanchez-Benavides, G., Falcon, C., Gramunt, N., Brugulat-Serrat, A., Grau, O., Gispert, J.D., Study, A, 2018a. Episodic memory and executive functions in cognitively healthy individuals display distinct neuroanatomical correlates which are differentially modulated by aging. Hum. Brain Mapp. 39, 4565–4579.

Cacciaglia, R., Molinuevo, J.L., Falcon, C., Brugulat-Serrat, A., Sanchez-Benavides, G., Gramunt, N., Esteller, M., Moran, S., Minguillon, C., Fauria, K., Gispert, J.D., 2018b. Effects of APOE-epsilon4 allele load on brain morphology in a cohort of middle-aged healthy individuals with enriched genetic risk for Alzheimer's disease. Alzheimers Dement. 14, 902–912.

Caselli, R.J., Dueck, A.C., Osborne, D., Sabbagh, M.N., Connor, D.J., Ahern, G.L., Baxter, L.C., Rapcsak, S.Z., Shi, J., Woodruff, B.K., Locke, D.E., Snyder, C.H., Alexander, G.E., Rademakers, R., Reiman, E.M., 2009. Longitudinal modeling of age-related memory decline and the APOE epsilon4 effect. N. Engl. J. Med. 361, 255–263.

Caselli, R.J., Dueck, A.C., Locke, D.E., Hoffman-Snyder, C.R., Woodruff, B.K., Rapcsak, S.Z., Reiman, E.M., 2011. Longitudinal modeling of frontal cognition in APOE epsilon4 homozygotes, heterozygotes, and noncarriers. Neurology 76, 1383–1388.

Chang, L., Douet, V., Bloss, C., Lee, K., Pritchett, A., Jernigan, T.L., Akshoomoff, N., Murray, S.S., Frazier, J., Kennedy, D.N., Amaral, D.G., Gruen, J., Kaufmann, W.E., Casey, B.J., Sowell, E., Ernst, T., Pediatric Imaging, N., Genetics Study, C, 2016. Gray matter maturation and cognition in children with different APOE epsilon genotypes. Neurology 87, 585–594.

Clarke, G.M., Anderson, C.A., Pettersson, F.H., Cardon, L.R., Morris, A.P., Zondervan, K.T., 2011. Basic statistical analysis in genetic case-control studies. Nat. Protoc. 6, 121–133.

Colom, R., Jung, R.E., Haier, R.J., 2007. General intelligence and memory span: evidence for a common neuroanatomic framework. Cogn Neuropsychol 24, 867–878.

Corder, E.H., et al., 1993. Gene dose of apolipoprotein E type 4 allele and the risk of Alzheimer's disease in late onset families. Science 261, 921–923.

Cosentino, S., Brickman, A.M., Griffith, E., Habeck, C., Cines, S., Farrell, M., Shaked, D., Huey, E.D., Briner, T., Stern, Y., 2015. The right insula contributes to memory awareness in cognitively diverse older adults. Neuropsychologia 75, 163–169.

Croxson, P.L., Browning, P.G., Gaffan, D., Baxter, M.G., 2012. Acetylcholine facilitates recovery of episodic memory after brain damage. J. Neurosci. 32, 13787–13795.

Dean 3rd, D.C., Jerskey, B.A., Chen, K., Protas, H., Thiyyagura, P., Roontiva, A., O'Muircheartaigh, J., Dirks, H., Waskiewicz, N., Lehman, K., Siniard, A.L., Turk, M.N., Hua, X., Madsen, S.K., Thompson, P.M., Fleisher, A.S., Huentelman, M.J., Deoni, S.C., Reiman, E.M., 2014. Brain differences in infants at differential genetic risk for late-onset Alzheimer disease: a cross-sectional imaging study. JAMA Neurol 71, 11–22.

Elias, M.F., Beiser, A., Wolf, P.A., Au, R., White, R.F., D'Agostino, R.B., 2000. The preclinical phase of alzheimer disease: a 22-year prospective study of the Framingham cohort. Arch. Neurol. 57, 808–813.

Elman, J.A., Oh, H., Madison, C.M., Baker, S.L., Vogel, J.W., Marks, S.M., Crowley, S., O'Neil, J.P., Jagust, W.J., 2014. Neural compensation in older people with brain amyloid-beta deposition. Nat. Neurosci. 17, 1316–1318.

Espeseth, T., Westlye, L.T., Walhovd, K.B., Fjell, A.M., Endestad, T., Rootwelt, H., Reinvang, I., 2012. Apolipoprotein E epsilon4-related thickening of the cerebral cortex modulates selective attention. Neurobiol. Aging 33 (304–322), e301.

Evans, S., Dowell, N.G., Tabet, N., Tofts, P.S., King, S.L., Rusted, J.M., 2014. Cognitive and neural signatures of the APOE E4 allele in mid-aged adults. Neurobiol. Aging 35, 1615–1623.

Farrer, L.A., et al., 1997. Effects of age, sex, and ethnicity on the association between apolipoprotein E genotype and Alzheimer disease. A meta-analysis. APOE and Alzheimer Disease Meta Analysis Consortium. JAMA 278, 1349–1356.

Filippini, N., Rao, A., Wetten, S., Gibson, R.A., Borrie, M., Guzman, D., Kertesz, A., Loy-English, I., Williams, J., Nichols, T., Whitcher, B., Matthews, P.M., 2009. Anatomically-distinct genetic associations of APOE epsilon4 allele load with regional cortical atrophy in Alzheimer's disease. Neuroimage 44, 724–728.

Filippini, N., Ebmeier, K.P., MacIntosh, B.J., Trachtenberg, A.J., Frisoni, G.B., Wilcock, G.K., Beckmann, C.F., Smith, S.M., Matthews, P.M., Mackay, C.E., 2011. Differential effects of the APOE genotype on brain function across the lifespan. Neuroimage 54, 602–610.

Fouquet, M., Besson, F.L., Gonneaud, J., La Joie, R., Chetelat, G., 2014. Imaging brain effects of APOE4 in cognitively normal individuals across the lifespan. Neuropsychol. Rev. 24, 290–299.

Gaskin, C.J., Happell, B., 2014. On exploratory factor analysis: a review of recent evidence, an assessment of current practice, and recommendations for future use. Int. J. Nurs. Stud. 51, 511–521.

George, S., Mufson, E.J., Leurgans, S., Shah, R.C., Ferrari, C., deToledo-Morrell, L., 2011. MRI-based volumetric measurement of the substantia innominata in amnestic MCI and mild AD. Neurobiol. Aging 32, 1756–1764.

Ghetti, S., Bunge, S.A., 2012. Neural changes underlying the development of episodic memory during middle childhood. Dev Cogn Neurosci 2, 381–395.

Gispert, J.D., Rami, L., Sanchez-Benavides, G., Falcon, C., Tucholka, A., Rojas, S., Molinuevo, J.L., 2015. Nonlinear cerebral atrophy patterns across the Alzheimer's disease continuum: impact of APOE4 genotype. Neurobiol. Aging 36, 2687–2701.

Gonneaud, J., Arenaza-Urquijo, E.M., Fouquet, M., Perrotin, A., Fradin, S., de La Sayette, V., Eustache, F., Chetelat, G., 2016. Relative effect of APOE epsilon4 on neuroimaging biomarker changes across the lifespan. Neurology 87, 1696–1703.

Good, C.D., Johnsrude, I.S., Ashburner, J., Henson, R.N., Friston, K.J., Frackowiak, R.S., 2001. A voxel-based morphometric study of ageing in 465 normal adult human brains. Neuroimage 14, 21–36.

Gramunt, N., Sanchez-Benavides, G., Buschke, H., Dieguez-Vide, F., Pena-Casanova, J., Masramon, X., Fauria, K., Gispert, J.D., Molinuevo, J.L., 2016. The memory binding test: development of two alternate forms into Spanish and Catalan. J. Alzheimers Dis. 52, 283–293.

Grothe, M., Heinsen, H., Teipel, S., 2013. Longitudinal measures of cholinergic forebrain atrophy in the transition from healthy aging to Alzheimer's disease. Neurobiol. Aging 34, 1210–1220.

Hall, A.M., Moore, R.Y., Lopez, O.L., Kuller, L., Becker, J.T., 2008. Basal forebrain atrophy is a presymptomatic marker for Alzheimer's disease. Alzheimers Dement. 4, 271–279.

Han, S.D., Bondi, M.W., 2008. Revision of the apolipoprotein E compensatory mechanism recruitment hypothesis. Alzheimers Dement. 4, 251–254.

Hanyu, H., Asano, T., Sakurai, H., Tanaka, Y., Takasaki, M., Abe, K., 2002. MR analysis of the substantia innominata in normal aging, Alzheimer disease, and other types of dementia. AJNR Am. J. Neuroradiol. 23, 27–32.

Honea, R.A., Vidoni, E., Harsha, A., Burns, J.M., 2009. Impact of APOE on the healthy aging brain: a voxel-based MRI and DTI study. J. Alzheimers Dis. 18, 553–564.

Jack Jr., C.R., Bennett, D.A., Blennow, K., Carrillo, M.C., Dunn, B., Haeberlein, S.B., Holtzman, D.M., Jagust, W., Jessen, F., Karlawish, J., Liu, E., Molinuevo, J.L., Montine, T., Phelps, C., Rankin, K.P., Rowe, C.C., Scheltens, P., Siemers, E., Snyder, H.M., Sperling, R., Contributors, 2018. NIA-AA research framework: toward a biological definition of Alzheimer's disease. Alzheimers Dement. 14, 535–562.

Jansen, W.J., Ossenkoppele, R., Knol, D.L., Tijms, B.M., Scheltens, P., et al., 2015. Prevalence of cerebral amyloid pathology in persons without dementia: a meta-analysis. JAMA 313, 1924–1938.

Jochemsen, H.M., Muller, M., van der Graaf, Y., Geerlings, M.I., 2012. APOE epsilon4 differentially influences change in memory performance depending on age. The SMART-MR study. Neurobiol Aging 33 (832), e815–e822.

Kantarci, K., Lowe, V., Przybelski, S.A., Weigand, S.D., Senjem, M.L., Ivnik, R.J., Preboske, G.M., Roberts, R., Geda, Y.E., Boeve, B.F., Knopman, D.S., Petersen, R.C., Jack Jr., C.R., 2012. APOE modifies the association between Abeta load and cognition in cognitively normal older adults. Neurology 78, 232–240.

Kim, H., Daselaar, S.M., Cabeza, R., 2010. Overlapping brain activity between episodic memory encoding and retrieval: roles of the task-positive and task-negative networks. Neuroimage 49, 1045–1054.

Klein, T.A., Endrass, T., Kathmann, N., Neumann, J., von Cramon, D.Y., Ullsperger, M., 2007. Neural correlates of error awareness. Neuroimage 34, 1774–1781.

Kochunov, P., Coyle, T., Lancaster, J., Robin, D.A., Hardies, J., Kochunov, V., Bartzokis, G., Stanley, J., Royall, D., Schlosser, A.E., Null, M., Fox, P.T., 2010. Processing speed is correlated with cerebral health markers in the frontal lobes as quantified by neuroimaging. Neuroimage 49, 1190–1199.

Lange, K.L., Bondi, M.W., Salmon, D.P., Galasko, D., Delis, D.C., Thomas, R.G., Thal, L.J., 2002. Decline in verbal memory during preclinical Alzheimer's disease: examination of the effect of APOE genotype. J. Int. Neuropsychol. Soc. 8, 943–955.

Lim, Y.Y., Kalinowski, P., Pietrzak, R.H., Laws, S.M., Burnham, S.C., Ames, D., Villemagne, V.L., Fowler, C.J., Rainey-Smith, S.R., Martins, R.N., Rowe, C.C., Masters, C.L., Maruff, P.T., 2018. Association of beta-amyloid and Apolipoprotein E epsilon4 with memory decline in preclinical Alzheimer Disease. JAMA Neurol 75, 488–494.

Liu, C.C., Kanekiyo, T., Xu, H., Bu, G., 2013. Apolipoprotein E and Alzheimer disease: risk, mechanisms and therapy. Nat. Rev. Neurol. 9, 106–118.

Matura, S., Prvulovic, D., Hartmann, D., Scheibe, M., Sepanski, B., Butz, M., Oertel-Knochel, V., Knochel, C., Karakaya, T., Fusser, F., Hattingen, E., Pantel, J., 2016. Age-related effects of the apolipoprotein E gene on brain function. J. Alzheimers Dis. 52, 317–331.

Mesulam, M.M., 2004. The cholinergic innervation of the human cerebral cortex. Prog. Brain Res. 145, 67–78.

Molinuevo, J.L., Gramunt, N., Gispert, J.D., Fauria, K., Esteller, M., Minguillon, C., Sanchez-Benavides, G., Huesa, G., Moran, S., Dal-Re, R., Cami, J., 2016. The ALFA project: a research platform to identify early pathophysiological features of Alzheimer's disease. Alzheimers Dement (N Y) 2, 82–92.

Mondadori, C.R., de Quervain, D.J., Buchmann, A., Mustovic, H., Wollmer, M.A., Schmidt, C.F., Boesiger, P., Hock, C., Nitsch, R.M., Papassotiropoulos, A., Henke, K., 2007. Better memory and neural efficiency in young apolipoprotein E epsilon4 carriers. Cereb. Cortex 17, 1934–1947.

Mowrey, W.B., Lipton, R.B., Katz, M.J., Ramratan, W.S., Loewenstein, D.A., Zimmerman, M.E., Buschke, H., 2016. Memory binding test predicts incident amnestic mild cognitive impairment. J. Alzheimers Dis. 53, 1585–1595.

Murphy, C., Jefferies, E., Rueschemeyer, S.A., Sormaz, M., Wang, H.T., Margulies, D.S., Smallwood, J., 2018. Distant from input: evidence of regions within the default mode network supporting perceptually-decoupled and conceptually-guided cognition. Neuroimage 171, 393–401.

Nao, J., Sun, H., Wang, Q., Ma, S., Zhang, S., Dong, X., Ma, Y., Wang, X., Zheng, D., 2017. Adverse effects of the Apolipoprotein E epsilon4 allele on episodic memory, task switching and Gray matter volume in healthy young adults. Front. Hum. Neurosci. 11, 346.

O'Donoghue, M.C., Murphy, S.E., Zamboni, G., Nobre, A.C., Mackay, C.E., 2018. APOE genotype and cognition in healthy individuals at risk of Alzheimer's disease: a review. Cortex 104, 103–123.

Operto, G., Cacciaglia, R., Grau-Rivera, O., Falcon, C., Brugulat-Serrat, A., Rodenas, P., Ramos, R., Moran, S., Esteller, M., Bargallo, N., Molinuevo, J.L., Gispert, J.D., Study, A, 2018. White matter microstructure is altered in cognitively normal middle-aged APOE-epsilon4 homozygotes. Alzheimers Res. Ther. 10, 48.

Papp, K.V., Amariglio, R.E., Mormino, E.C., Hedden, T., Dekhytar, M., Johnson, K.A., Sperling, R.A., Rentz, D.M., 2015. Free and cued memory in relation to biomarker-defined abnormalities in clinically normal older adults and those at risk for Alzheimer's disease. Neuropsychologia 73, 169–175.

Parvaz, M.A., Maloney, T., Moeller, S.J., Malaker, P., Konova, A.B., Alia-Klein, N., Goldstein, R.Z., 2014. Multimodal evidence of regional midcingulate gray matter volume underlying conflict monitoring. Neuroimage Clin 5, 10–18.

Protas, H.D., Chen, K., Langbaum, J.B., Fleisher, A.S., Alexander, G.E., Lee, W., Bandy, D., de Leon, M.J., Mosconi, L., Buckley, S., Truran-Sacrey, D., Schuff, N., Weiner, M.W., Caselli, R.J., Reiman, E.M., 2013. Posterior cingulate glucose metabolism, hippocampal glucose metabolism, and hippocampal volume in cognitively normal, late-middle-aged persons at 3 levels of genetic risk for Alzheimer disease. JAMA Neurol 70, 320–325.

Ray, N.J., Metzler-Baddeley, C., Khondoker, M.R., Grothe, M.J., Teipel, S., Wright, P., Heinsen, H., Jones, D.K., Aggleton, J.P., O'Sullivan, M.J., 2015. Cholinergic basal forebrain structure influences the reconfiguration of white matter connections to support residual memory in mild cognitive impairment. J. Neurosci. 35, 739–747.

Reiman, E.M., Chen, K., Alexander, G.E., Caselli, R.J., Bandy, D., Osborne, D., Saunders, A.M., Hardy, J., 2004. Functional brain abnormalities in young adults at genetic risk for late-onset Alzheimer's dementia. Proc. Natl. Acad. Sci. U. S. A. 101, 284–289.

Reiman, E.M., Chen, K., Alexander, G.E., Caselli, R.J., Bandy, D., Osborne, D., Saunders, A.M., Hardy, J., 2005. Correlations between apolipoprotein E epsilon4 gene dose and brain-imaging measurements of regional hypometabolism. Proc. Natl. Acad. Sci. U. S. A. 102, 8299–8302.

Reiman, E.M., Chen, K., Liu, X., Bandy, D., Yu, M., Lee, W., Ayutyanont, N., Keppler, J., Reeder, S.A., Langbaum, J.B., Alexander, G.E., Klunk, W.E., Mathis, C.A., Price, J.C., Aizenstein, H.J., DeKosky, S.T., Caselli, R.J., 2009. Fibrillar amyloid-beta burden in cognitively normal people at 3 levels of genetic risk for Alzheimer's disease. Proc. Natl. Acad. Sci. U. S. A. 106, 6820–6825.

Rodrigo, A.H., Domenico, S.I., Ayaz, H., Gulrajani, S., Lam, J., Ruocco, A.C., 2014. Differentiating functions of the lateral and medial prefrontal cortex in motor response inhibition. Neuroimage 85 (Pt 1), 423–431.

Rodrigue, K.M., Kennedy, K.M., Devous Sr., M.D., Rieck, J.R., Hebrank, A.C., Diaz-Arrastia, R., Mathews, D., Park, D.C., 2012. beta-Amyloid burden in healthy aging: regional distribution and cognitive consequences. Neurology 78, 387–395.

Schmitz, T.W., Nathan Spreng, R., Alzheimer's Disease Neuroimaging, I., 2016. Basal forebrain degeneration precedes and predicts the cortical spread of Alzheimer's pathology. Nat. Commun. 7, 13249.

Schmitz, T.W., Mur, M., Aghourian, M., Bedard, M.A., Spreng, R.N., Alzheimer's Disease Neuroimaging, I., 2018. Longitudinal Alzheimer's degeneration reflects the spatial topography of cholinergic basal forebrain projections. Cell Rep. 24, 38–46.

Seeley, W.W., Menon, V., Schatzberg, A.F., Keller, J., Glover, G.H., Kenna, H., Reiss, A.L., Greicius, M.D., 2007. Dissociable intrinsic connectivity networks for salience processing and executive control. J. Neurosci. 27, 2349–2356.

Sohn, M.H., Albert, M.V., Jung, K., Carter, C.S., Anderson, J.R., 2007. Anticipation of conflict monitoring in the anterior cingulate cortex and the prefrontal cortex. Proc. Natl. Acad. Sci. U. S. A. 104, 10330–10334.

Sperling, R., Mormino, E., Johnson, K., 2014. The evolution of preclinical Alzheimer's disease: implications for prevention trials. Neuron 84, 608–622.

Tau, G.Z., Peterson, B.S., 2010. Normal development of brain circuits. Neuropsychopharmacology 35, 147–168.

Teipel, S.J., Flatz, W.H., Heinsen, H., Bokde, A.L., Schoenberg, S.O., Stockel, S., Dietrich, O., Reiser, M.F., Moller, H.J., Hampel, H., 2005. Measurement of basal forebrain atrophy in Alzheimer's disease using MRI. Brain 128, 2626–2644.

Ten Kate, M., Sanz-Arigita, E.J., Tijms, B.M., Wink, A.M., Clerigue, M., Garcia-Sebastian, M., Izagirre, A., Ecay-Torres, M., Estanga, A., Villanua, J., Vrenken, H., Visser, P.J., Martinez-Lage, P., Barkhof, F., 2016. Impact of APOE-varepsilon4 and family history of dementia on gray matter atrophy in cognitively healthy middle-aged adults. Neurobiol. Aging 38, 14–20.

Tuminello, E.R., Han, S.D., 2011. The apolipoprotein e antagonistic pleiotropy hypothesis: review and recommendations. Int. J. Alzheimers Dis. 2011, 726197.

Van Petten, C., 2004. Relationship between hippocampal volume and memory ability in healthy individuals across the lifespan: review and meta-analysis. Neuropsychologia 42, 1394–1413.

Wechsler, D., 2012. WAIS-IV, Escala de inteligencia de Wechsler para adultos-IV. Pearson, Madrid.

Wishart, H.A., Saykin, A.J., Rabin, L.A., Santulli, R.B., Flashman, L.A., Guerin, S.J., Mamourian, A.C., Belloni, D.R., Rhodes, C.H., McAllister, T.W., 2006. Increased brain activation during working memory in cognitively intact adults with the APOE epsilon4 allele. Am. J. Psychiatry 163, 1603–1610.

Wolf, A.B., Valla, J., Bu, G., Kim, J., LaDu, M.J., Reiman, E.M., Caselli, R.J., 2013.

Apolipoprotein E as a beta-amyloid-independent factor in Alzheimer's disease. Alzheimers Res. Ther. 5, 38.

Zaborszky, L., Hoemke, L., Mohlberg, H., Schleicher, A., Amunts, K., Zilles, K., 2008. Stereotaxic probabilistic maps of the magnocellular cell groups in human basal forebrain. Neuroimage 42, 1127–1141.

Zaborszky, L., Csordas, A., Mosca, K., Kim, J., Gielow, M.R., Vadasz, C., Nadasdy, Z., 2015. Neurons in the basal forebrain project to the cortex in a complex topographic organization that reflects corticocortical connectivity patterns: an experimental study based on retrograde tracing and 3D reconstruction. Cereb. Cortex 25, 118–137.

Zhao, N., Liu, C.C., Qiao, W., Bu, G., 2017. Apolipoprotein E, receptors, and modulation of Alzheimer's Disease. Biol. Psychiatry 83, 347–357.